PHILOSOPHICAL MAGAZINE A, 2000, VOL. 80, NO. 12, 2855–2870

# The mechanics of slip transition at intermediate temperatures in ⟨001⟩-oriented NiAl single crystals II. A metastable state for $a\langle 111\rangle\{110\}$ dislocations in NiAl and its role in their decomposition

J. BROWN†, R. SRINIVASAN‡, M. J. MILLS‡ and M. S. DAW†§||

† Department of Physics and Astronomy, Clemson University, Clemson, South Carolina, USA
‡ Department of Materials Science and Engineering, The Ohio State University, Columbus, Ohio 43210, USA
§ Computational Materials Group, Motorola, 0501 Ed Bluestein Boulevard, MD K10, Austin, Texas 78721, USA

[*Received 25 October 1999 and accepted in revised form 7 February 2000*]

ABSTRACT

We show in this paper that there exists a metastable arrangement of products in the reaction $a\langle 111\rangle \rightarrow a\langle 110\rangle + a\langle 001\rangle$ in B2 NiAl. Atomistic calculations show that the metastable state can be formed spontaneously by a local shuffle or climb decomposition. Once formed, the 'piggyback' configuration can glide as a unit, with a restoring force helping to keep it intact. However, if the product lines become separated locally beyond a critical distance, the result is a decomposition loop. Small dislocation loops (less than 100 Å) collapse, large loops (greater than 3000 Å) evolve into dislocation dipoles, and medium loops can fail to evolve further. These results are consistent with detailed observations of the microstructure. The implications for this metastable state for the mechanical properties are examined.

## § 1. INTRODUCTION

Ordered intermetallic alloys can exhibit peculiar deformation behaviour, such as the anomalous temperature dependence of the yield stress. This behaviour has been naturally linked to the intriguing complexities of the slip modes.

As described in detail in the accompanying paper (Srinivasan *et al*. 2000), the B2-type intermetallic NiAl exhibits a plateau in the yield stress versus temperature when deformed uniaxially along a cube axis, the so-called 'hard orientation' (Srinivasan *et al*. 1996). The yield stress drops abruptly above a transition (or 'knee') temperature $T_k$, of the order of 600–800 K. Below $T_k$, deformation occurs on the $a\langle 111\rangle\{110\}$ slip system, where $a = 2.88$ Å, the lattice constant of stoichiometric NiAl. Several experiments have correlated the 'knee' with a transition from $a\langle 111\rangle$ to non-$a\langle 111\rangle$ slip (Kim 1990, Field *et al*. 1991, Kim and Gibala 1991, Srinivasan *et al*. 1996).

The decomposition reaction $a\langle 111\rangle \rightarrow a\langle 110\rangle + a\langle 001\rangle$ is predicted to occur for NiAl by elasticity theory (Yoo *et al*. 1990, Fu and Yoo 1992). For a broad range of

|| Email: murray_daw@email.sps.mot.com.

*Philosophical Magazine* A ISSN 0141–8610 print/ISSN 1460-6992 online 
http://www.tandf.co.uk/journals

character encompassing edge orientation, the reaction is energetically favourable and can occur by simple glide on the parent {110} glide plane.

While the elasticity results explain the eventual decomposition of $a\langle 111\rangle$ dislocations, the mystery remains as to why the decomposition is postponed to a temperature of around 800 K in Ni–44 at.% Al. Energetically, the decomposition would be expected at low temperatures; one would not expect long line lengths of $a\langle 111\rangle$ dislocations near edge character. However, the microstructural observations detailed in the accompanying paper (Srinivasan *et al.* 2000) clearly reveal $a\langle 111\rangle$ dislocations up to $T_k$, including those with near-edge character. In addition, a sequence of events has been postulated whereby the $a\langle 111\rangle$ dislocation decomposes into $a\langle 110\rangle + a\langle 001\rangle$ at intermediate temperatures (near 800 K). The decomposition is observed to begin along a small piece of the line. Contrary to what one might expect based on energetics, the decomposition does not proceed by extending itself along the line, thereby unzipping the remaining $a\langle 111\rangle$. Rather, the length of decomposed segment remains fairly constant, and the $a\langle 001\rangle$ child is extended indefinitely in the form of a dipole. Again, the resistance of the $a\langle 111\rangle$ to decomposition, even after the decomposition has been nucleated, seems surprising.

Further experimental work (Srinivasan *et al.* 2000) has revealed the details of the decomposition as well as a significant stoichiometry dependence. Ni-rich material (Ni–44 at.% Al) shows a transition at 800 K. At 750 K for low strains, the near-edge $a\langle 111\rangle$ dislocations show cusps which appear to be of lower mobility. Repeating the experiment 50 K higher shows that the cusps have developed into the decomposition dipoles (see figure 5 of Srinivasan *et al.* (2000)). Finally, deformation at 800 K reveals that the decomposition has run to completion; only $a\langle 111\rangle$ and $a\langle 001\rangle$ dislocations are observed. In addition, many of the $a\langle 001\rangle$ dislocations are arrayed in dipoles.

This paper will offer an explanation of these observations. We shall show, based on both atomistic and continuum calculations, that a metastable structure for the $a\langle 111\rangle$ can form spontaneously. This metastable state is mobile on the {110} plane and resists decomposition up to high temperatures. We shall analyse the possible pathways for decomposition of this metastable structure and show that the path is entirely consistent with the $a\langle 001\rangle$ dipoles seen in the experiments.

The remainder of this paper is organized as follows. In the next section, we shall discuss the theoretical considerations which provide evidence for the existence of a metastable state, mobile on the {110} glide plane. In § 3, we shall analyse the pathways for decomposition from the metastable state and compare with experimental results. We shall then discuss the implications of these findings and summarize in the conclusions.

## § 2. A NEW METASTABLE STATE FOR THE $a[111]$ DISLOCATION

Let us consider a dislocation loop with Burgers vector $a[111]$ on the $(1\bar{1}0)$ plane. As noted by Yoo *et al.* (1990) and Fu and Yoo (1992), the anisotropic elastic energy is reduced if the near-edge portions decompose: $a[111] \rightarrow a[110] + a[001]$. For the near-screw line direction, the decomposition is energetically uphill. The line directions dividing the near-edge behaviour from near-screw behaviour are [110] and [001], for which the reaction is energetically neutral, according to elasticity theory. These considerations led Yoo *et al.* to expect a glide decomposition of the edge-like portions of an $a[111]$ loop. Such decomposition would be expected to occur spontaneously at any temperature.

It is also possible, as noted by Yoo *et al.* that the $a[111]$ could dissociate: $a[111] \rightarrow (a/2)[111] + (a/2)[111]$. Such dissociation has not been seen experimentally for NiAl for any character, presumably because the antiphase boundary energy for this highly ordered alloy is too high to allow for a significant dissociation.

The picture described by Yoo *et al.* is not borne out completely in experiment. Rather, near-edge $a[111]$ dislocations are observed (in Ni–44 at.% Al) quite prevalently up to 750 K. It is difficult to reconcile these two apparently contradictory facts, because it is difficult to impugn either.

As though to add to the complexity, the $a[111]$ is observed to decompose, but only when the temperature exceeds 750 K. In that case, the decomposition is observed to occur by the nucleation of a locally decomposed portion. For temperatures just at the knee and for small strains, the decomposition is observed only by the cusp-like appearance of $a[111]$ dislocations; the cusps are presumably short decomposed segments. For higher temperatures, the decomposed portions are clearly resolved in the form of a decomposition half-loop, with $a[110]$ and $a[001]$ legs. When pushed to higher strains, the decomposition appears to proceed to completion, leaving $a[110]$ and $a[001]$ products. Many of the $a[001]$ products are arranged in dipoles. Interestingly, the line direction observed for the decomposed portions is $[11\bar{1}]$, which is of mixed character.

Clearly the observations are not totally consistent with the elasticity results of Yoo *et al.* The decomposition, which should occur spontaneously at any temperature, is instead observed to be delayed to high temperatures. Instead of occurring there in a straightforward way, the decomposition proceeds via a nucleation event which evolves in a unique fashion.

In the remainder of this section we present the theoretical evidence for the existence of a metastable configuration for the $a\langle 111\rangle$ which is part of the way towards decomposition. This metastable state has not been appreciated in previous atomistic or continuum calculations. We consider in the following sections the driving forces and mechanism by which a metastable state for the $a\langle 111\rangle$ can be produced. First, in § 2.1 we show that the energetics of the elastic medium favour the creation of the metastable state. In the subsequent § 2.2, we show that the atomistics of the core region allow it to occur. Finally, in § 3, we shall study the process by which this metastable state decomposes.

In subsequent sections, we shall establish the possibility that the decomposition could occur *perpendicular* to the glide plane; that is, suppose that short-range climb occurs to separate the products on to neighbouring parallel $(1\bar{1}0)$ glide planes. The resulting configuration is illustrated in figure 1. The glide plane of the $a[001]$ dislocation is one or two planes above (or below) that of the $a[110]$.

Clearly, significant climb is not possible in the absence of diffusion but, in this case, to separate the products by one or two planes would require only a local reshuffle that might occur spontaneously. Such a configuration is metastable (at best) with respect to complete decomposition.

### 2.1. *Elastic continuum considerations*

There are two contributions to the elastic strain energy which drive the formation of the metastable state. First, the same elastic forces which favour glide decomposition also act in the climb direction, pushing against the products in the direction perpendicular to the glide plane. Second, the external uniaxial compression (or tension) along a cube axis forces the products apart (that is the external climb forces

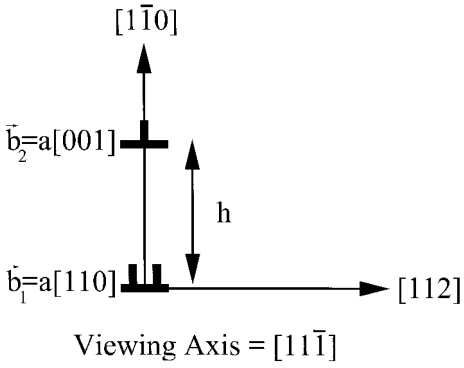


Figure 1. The idealized metastable state of the $a[111]$ dislocation along the $[11\bar{1}]$ line direction. The decomposition $a[111] \rightarrow a[110] + a[001]$ has occurred perpendicular to the glide plane, separating the products by a distance $h$ in the climb direction.

are unequal). If a short-ranged reshuffling can occur, then the elastic energy should be lowered.

The products $a[110]$ and $a[001]$ exert a radial force on each other which depends on the character. Consider two parallel, straight dislocations with $\mathbf{b}_1 = a[110]$ and $\mathbf{b}_2 = a[001]$, in the $(1\bar{1}0)$ plane. The resulting expressions are simplest if we define the line direction by $\hat{\xi} = (\cos\theta)[110]/2^{1/2} + (\sin\theta)[001]$. (Keep in mind that, with this definition, the screw orientation occurs at $\theta = 35.26^\circ$.) Isotropic theory (Hirth and Lothe 1982) shows that the radial component of the force (per unit length) between them is

$$f_r = -\frac{\mu\nu b_1 b_2}{4\pi(1-\nu)R}\sin(2\theta), \tag{1}$$

where $\mu$ and $\nu$ are the (Voigt-averaged) isotropic shear modulus and Poisson's ratio respectively. This is repulsive over one half of the possible line directions (edge like), and attractive for the other half (screw like). In isotropic theory, the radial force is independent of the relative orientation of the products and so can act to push the products either along the glide plane or perpendicular to the glide plane. In figure 2, we show the radial force (for climb decomposition) calculated with anisotropic theory (Hirth and Lothe 1982), showing the same qualitative behaviour as for isotropic theory. Thus, edge-like character has an intrinsic force which tends to push the products apart.

As an additional aid to separation, the external stress state in the 'hard orientation' gives rise to unequal climb forces. For the $(1\bar{1}0)$ slip plane, the climb force (Hirth and Lothe 1982) on $\mathbf{b}_1 = a[110]$ is $b_1|\sin\theta|(\sigma_{xx} + \sigma_{yy})/2$, and the climb force on $\mathbf{b}_2 = a[001]$ is $b_2|\cos\theta|\sigma_{zz}$. Note that the hard-oriented stress here refers to stress along the [100] or [010] axes, since only these two axes offer a resolved shear stress on the $a[111](1\bar{1}0)$ system.

These two driving forces can both contribute to a separation of the products in the climb direction. In the next section we examine the results of atomic-scale calculations to see whether the system can take advantage of these driving forces.

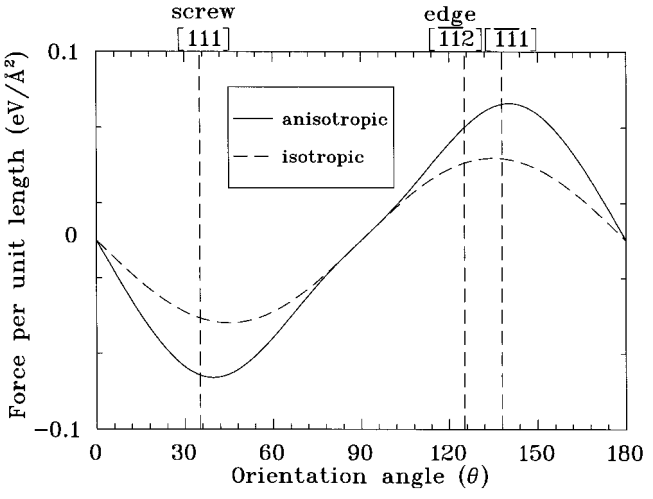


Figure 2. The radial force between $\mathbf{b}_1 = a[110]$ and $\mathbf{b}_2 = a[001]$ for various line directions in the $(1\bar{1}0)$ plane. The angle $\theta$ is defined relative to the [110] direction (see text before equation (1)). The results are plotted for anisotropic and (Voigt-averaged) isotropic elastic media. The products are oriented perpendicular to the glide plane (see figure 1) and are separated by 4 Å. The analytical form for the isotropic case is given by equation (1) in the text.

### 2.2. *Atomistics*

Given the tendency of the products to climb apart, it remains to be seen whether a local reshuffling can be accomplished to reduce the energy. Such a question is best answered by detailed atomistic calculations. Interestingly, very few such calculations have been done for the $a[111]$ dislocation with near-edge character (Rao *et al.* 1991, Schroll *et al.* 1998a,b). None has been done for the $[11\bar{1}]$ line direction which is suggested by the observations.

We therefore carried out calculations of the $a[111](1\bar{1}0)$ dislocation along $[11\bar{1}]$. In figure 3 we show the initial configuration. The calculations were performed using the embedded-atom method (EAM). For comparison purposes, we performed parallel calculations using two separate potentials: firstly, that of Rao *et al.* (1991) and, secondly, that of Ludwig and Gumbsch (1995). The calculation was done on a cylinder of material, periodic along the axis of the cylinder, with atoms along the surface of the cylinder fixed at their initial positions and the remainder free to move to minimize the energy. The initial positions were determined by displacing the atoms of a perfect lattice according to the displacement field solution for dislocations in linear anisotropic elasticity theory. The singularity and cut of the solutions were carefully placed between atomic positions and planes.

In doing the optimization, we found evidence of many minima. The minimum that was found by the optimization was sensitive to the optimization procedure and to the details of the initial condition. To find the lowest-energy state, we explored a variety of optimization techniques (conjugate gradients, damped molecular dynamics, and molecular dynamics at temperature followed by a quench) and initial conditions (slight variations in the placement of the centre of the dislocation). In the end, we found that there is indeed one clearly defined lowest-energy configuration. This lowest-energy state was most easily obtained by a simple annealing procedure,

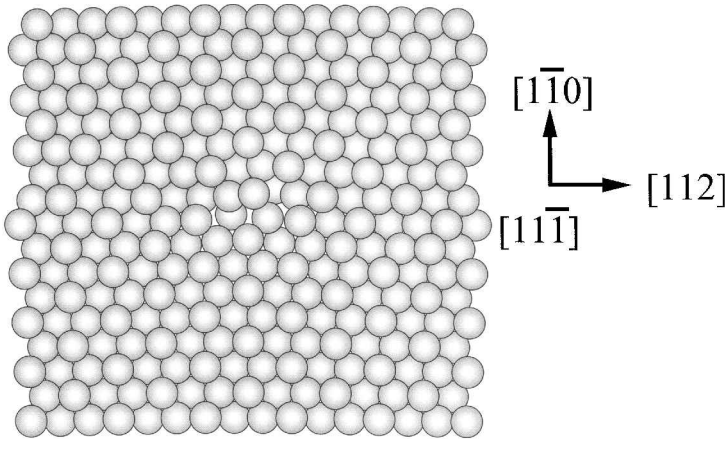


Figure 3. The starting atomistic positions for the $a[111](1\bar{1}0)$ dislocation with the $[11\bar{1}]$ line direction. The viewing axis is along the line direction, with the horizontal direction taken along the glide direction.

where one starts with the ideal geometry of figure 3, performs a molecular dynamics calculation at 600 K for 50 ps and then does a conjugate gradient minimization.

In figure 4, we show the resulting relaxed configuration, together with the displacements relative to the initial structure. In figure 4 (*b*) the in-plane displacements are shown relative to the starting position. Clearly the local reshuffling has resulted in a climb-decomposed configuration. The $a[001]$ product has separated from the $a[110]$ along the $[1\bar{1}0]$ direction by approximately 6 Å. The screw displacements associated with the relaxed configuration are shown in figure 4 (*c*), which is a cut normal to the [112] glide *direction*. The screw displacements are consistent with the proposed climb-decomposed configuration. Because this was a short molecular dynamics run, no long-range diffusion can occur. Rather, the local reshuffling has accomplished the climb without diffusion.

## § 3. Decomposition of the metastable state

The metastable structure illustrated in figure 1 consists of two perfect dislocations gliding on parallel glide planes, separated by a climb distance $h$ of the order of two interplanar spacings. We shall show in this section that this structure is indeed metastable (not simply unstable), and we shall trace out the path by which it will decompose.

Consider, as in figure 5, that the products have become slightly separated by a distance $h$ along the climb direction. (Remember, by our previous investigation, we are restricting our considerations to near-edge orientations; see equation (1).) The work required to separate the products a distance $L$ along the *glide* direction, as illustrated in figure 5, is

$$\varepsilon = \frac{\mu a^2}{2^{3/2}\pi(1-\nu)}\left[\nu \ln\left(\frac{(h^2+L^2)^{1/2}}{h}\right) - \frac{L^2}{h^2+L^2}\right]\sin(2\theta). \tag{2}$$

(Recall that $\theta$ is the angle the line direction makes with the [110] direction.) The energy of this glide separation is plotted in figure 6 (*a*) as a function of $L$ for the $[11\bar{1}]$

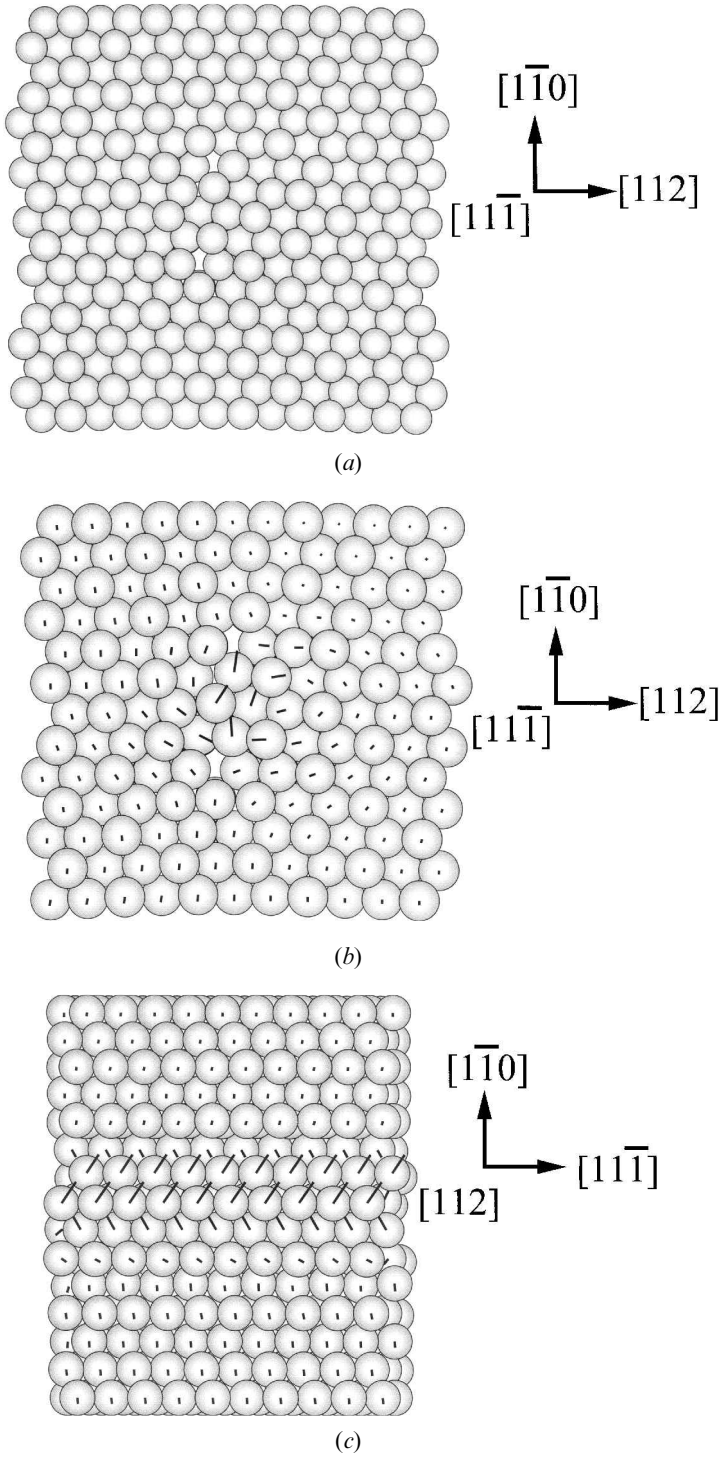


Figure 4. (*a*) The relaxed atomistic positions obtained from the initial condition shown in figure 3. (*b*) The same, showing the in-plane displacements relative to the starting position. (*c*) The same again, but with the viewing axis now from the glide direction. The line direction is now horizontal. This view shows the screw components.

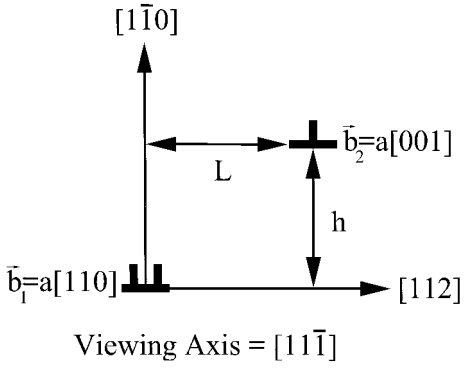


Figure 5. The metastable state after glide separation of its components. The products are separated by a distance $h$ along the climb direction and $L$ along the glide direction. Compare with figure 1.

line direction. For $L$ less than a distance of about $2h$, the elastic medium exerts a restoring force which tends to realign the products along the vertical. However, beyond a certain distance, the energy starts to decrease and the decomposition proceeds unbounded, consistent with the positive radial force in equation (1). This behaviour is summarized in figure 6(*b*) where the line $L \approx 2h$ separates regions in the $h$–$L$ plane where it is energetically favourable for products to revert to a purely climb-decomposed configuration or one that includes both climb and glide separations.

The metastable minimum occurs for a whole range of edge-like line directions. In fact, there is a metastable *minimum* in the interaction energy precisely along those line directions for which there is a *repulsive* radial force (see equation (1)). For screw-like orientations, by contrast, the radial force component resists any decomposition whatsoever.

The energy barrier (per unit length) occurs at $L_b = h(2/\nu - 1)^{1/2}$ and is of height

$$\varepsilon_b = \frac{\mu a^2}{4 \times 2^{1/2}\pi(1-\nu)} \left[-2 + \nu - \nu \ln\left(\frac{\nu}{2}\right)\right] \sin(2\theta). \tag{3}$$

It is interesting to note that $L_b$ is independent of $\theta$ and $\varepsilon_b$ is independent of $h$!

The energetics as calculated from anisotropic elasticity theory are also plotted in figure 6(*a*), showing that the qualitative form is obtained by isotropic theory, although the energy barrier calculated by isotropic theory is a factor of nearly two too high.

Clearly, however, the decomposition cannot proceed directly by the separation of two straight product dislocations; the energy for that would be proportional to their length. Rather, a much lower energy is required to push only a portion of the dislocation over the barrier, forming a section of the dislocation where the decomposition has occurred only locally.

To conduct a more precise analysis, we consider the idealized configuration illustrated in figure 7, where the geometry has been simplified to rectilinear segments. In this ideal geometry, there is a parameter $L$ describing the excursion distance of a segment of length $W$. This is amenable to a straightforward application of isotropic

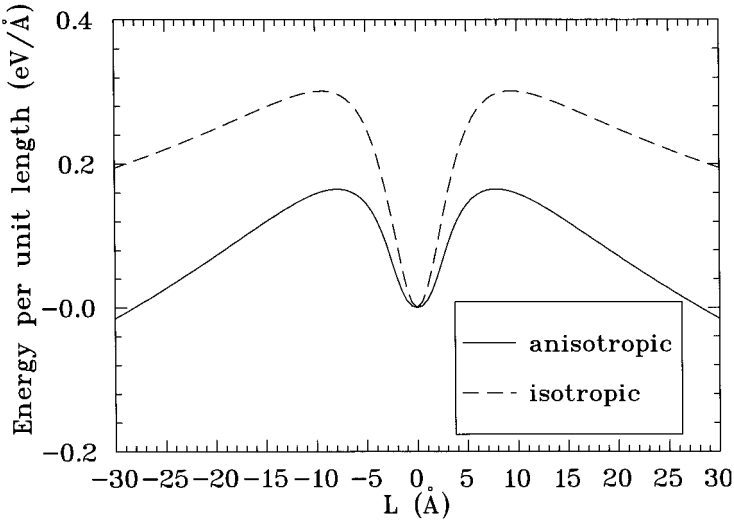


(*a*)

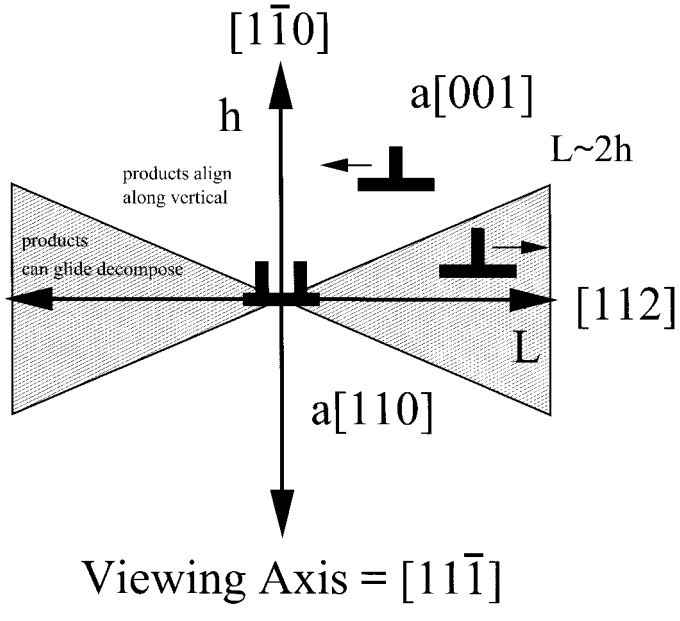


(*b*)

Figure 6. (*a*) The interaction energy (equation (2)) of the components shown in figure 5 versus $L$ for $h = 4$ Å. (*b*) Schematic diagram showing the range of stability of the climb-decomposed and climb-and-glide-decomposed $a[111]$ dislocation. For products climb decomposed by an amount $h$, further decomposition in the glide plane is energetically favourable in the shaded region, while the purely climb-decomposed configuration is favoured in the region that is not shaded. The maximum in the energy barrier is given by the equation $L \approx 2h$, where $L$ is the separation along the [11$\bar{2}$] edge line direction, and $h$ is the separation along the [1$\bar{1}$0] direction normal to the (1$\bar{1}$0) glide plane. The arrows near the $a[001]$ dislocation in each case show the direction of the interaction force between the $a[110]$ and $a[001]$ dislocations.

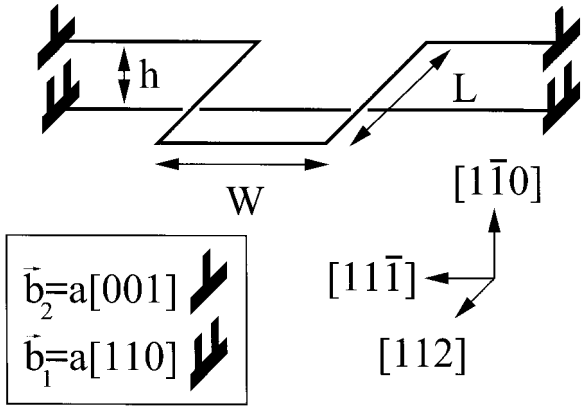


Figure 7. Idealized configuration leading from the metastable state to decomposition.

elasticity theory. The energy of this configuration can be obtained directly (Hirth and Lothe 1982) as

$$
\begin{aligned}
E(W,L) &= E_{\text{int}} + E_{\text{self}},\\
E_{\text{int}} &= \frac{a^2\mu W}{6(1-\nu)\pi}\left[\frac{2L^2}{h^2+L^2} + \nu \ln\left(\frac{h^2}{h^2+L^2}\right)\right],\\
E_{\text{self}} &= \frac{a^2\mu L(3-2\nu)}{6(1-\nu)\pi}\left[\ln\left(\frac{L}{r_0}\right) + g\left(\frac{W}{L}\right)\right],\\
g(r) &= -r + (1+r^2)^{1/2} - \ln\left(\frac{1+(1+r^2)^{1/2}}{r}\right)\\
&\quad + \frac{3-\nu}{3-2\nu}\left[-1-r+(1+r^2)^{1/2} + r\ln\left(\frac{2r}{r+(1+r^2)^{1/2}}\right)\right],
\end{aligned}
\tag{4}
$$

where $r \equiv W/L$, and $r_0$ is the inner cut-off distance.

The energy $E(W,L)$ has the asymptotic limits that we would expect. For large $W$, we recover interaction of straight dislocations expressed (for general line direction) in equation (2). For large $L$, we find the energy to be that of an $a[001]$ dipole separated by a distance $W$, which is attractive and goes like $\ln W$.

We now consider the evolution of the decomposition by evaluating the forces acting on the segments illustrated in figure 7. These forces are related to the derivatives of the energy in equation (4) with respect to the state parameters $W$ and $L$. We assume that a segment experiencing a net force will not move if that force is below the Peierls force and moves with the speed of sound in the direction of the force if the magnitude of the net force exceeds the Peierls force. This picture is greatly simplified, but it at least accounts for the major characteristics we expect.

The equations of motion determining the evolution of the parameters $W$ and $L$ are thus

$$\begin{aligned}\frac{\mathrm{d}W}{\mathrm{d}t} &= 2c\Theta(|f_W| - f_{\mathrm{P}}^{a[001]})\,\mathrm{sgn}\,(f_W),\\ \frac{\mathrm{d}L}{\mathrm{d}t} &= c\Theta(|f_{\mathrm{ext}}| - f_{\mathrm{P}}^{a[110]})\,\mathrm{sgn}\,(f_{\mathrm{ext}}) + c\Theta(|f_L| - f_{\mathrm{P}}^{a[001]})\,\mathrm{sgn}\,(f_L),\end{aligned} \tag{5}$$

where $c$ is the sound velocity, $\Theta$ is the unit step function,

$$\begin{aligned} f_W &= -\frac{1}{L}\frac{\mathrm{d}E(W,L)}{\mathrm{d}W},\\ f_L &= -\frac{1}{W}\frac{\mathrm{d}E(W,L)}{\mathrm{d}L},\\ f_{\mathrm{ext}} &= \sigma_{\mathrm{a}} b^{a[110]},\\ f_{\mathrm{P}}^{a[001]} &= \sigma_{\mathrm{P}}^{a[001]} b^{a[001]},\\ f_{\mathrm{P}}^{a[110]} &= \sigma_{\mathrm{P}}^{a[110]} b^{a[110]},\end{aligned} \tag{6}$$

$\sigma_{\mathrm{a}}$ is the applied 'hard-oriented' stress acting along the [010] direction, $\sigma_{\mathrm{P}}^{a[001]}$ is the Peierls frictional stress on the $a[001]$ dislocation, and $\sigma_{\mathrm{P}}^{a[110]}$ is the Peierls frictional stress on the $a[110]$, both in the $(1\bar{1}0)$ plane and along the $[11\bar{1}]$ direction.

From the experimental results (Srinivasan *et al.* 1998) on Ni-rich material (Ni–44 at.% Al), the resolved shear stress, at the temperature for which the decomposition is first observed, is reported to be $\sigma_{\mathrm{a}} = 0.75$ GPa. The force is applied only to the $a[110]$ segments, leaving no force on the $a[001]$ segments as would be the case for uniaxial deformation along the cube axis (hard orientation). The Peierls stresses are estimated to be $\sigma_{\mathrm{P}}^{a[110]} = 0.46$ GPa and $\sigma_{\mathrm{P}}^{a[001]} = 0.26$ GPa. The estimate for $\sigma_{\mathrm{P}}^{a[100]}$ is in agreement with EAM calculations of Schroll *et al.* (1998a,b). Schroll *et al.* also calculated the Peierls barriers for $a[110]$, but not for the $[11\bar{1}]$ direction.

The physics embodied in the equations of motion is quite simple. The force on each segment is compared with the frictional force; if the magnitude of the force exceeds the frictional force, it moves in the direction of the force.

For $W$, the situation is quite simple and is illustrated in figure 8. The dipole separation $W$ will decrease if the force $f_W$ on the segments is attractive and overcomes the Peierls force for $a[001]$ (region 1 in the figure). Similarly, the dipole separation $W$ will increase if $f_W$ is repulsive and overcomes the Peierls force for $a[001]$ (does not occur in the figure). If the magnitude of $f_W$ is less than the Peierls force, then $W$ is constant (region 2 in the figure).

For $L$, the consideration is slightly more subtle. $L$ is the parameter which characterizes the degree of decomposition and is the separation between the $a[110]$ and the $a[001]$ (see figure 7). The force on the $a[110]$ is the external force, because the $a[110]$ is constrained in our idealized geometry to be aligned with the infinite $a[111]$ parent which is driven by the external force. This external force is assumed to be greater than the frictional force; so the $a[110]$ is assumed always to be in motion. By contrast, there is no direct external force on the $a[001]$ segment parallel to the $a[110]$; the force on this segment is simply that which derives from its interaction with other segments (that is from equation (4)), which is $f_L$. If that force $f_L$ is weaker than the frictional force, then the $a[001]$ does not move; the $a[110]$ moves, leaving the $a[001]$ behind; so $L$ increases (region 2 in figure 9). If $f_L$ is repulsive and greater than the frictional force, $L$ grows rapidly (region 3 in figure 9). If $f_L$ is attractive and greater than the frictional force, $L$ remains constant (region 1 in figure 9). In this last case,

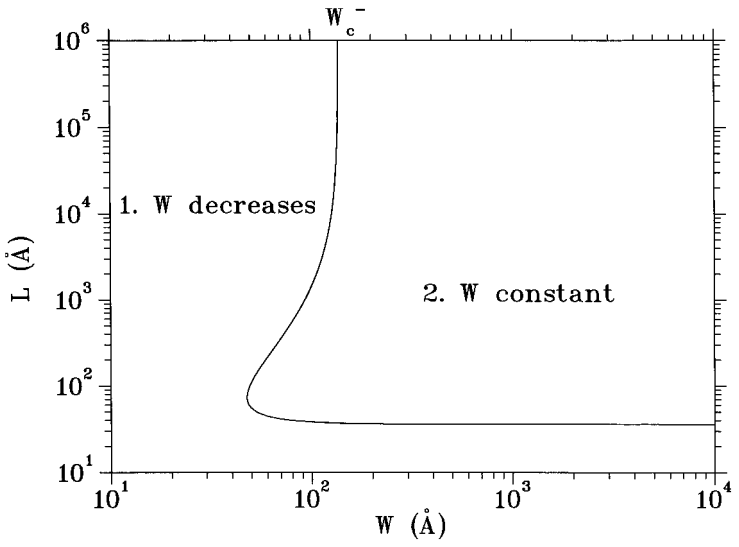


Figure 8. Contours of constant $f_W$, showing different regions of behaviour: region 1, $f_W < -f_P^{a[001]}$, $W$ decreases; region 2, $-f_P^{a[001]} < f_W < +f_P^{a[001]}$, $W$ is constant; region 3, $f_W > +f_P^{a[001]}$, $W$ increases (does not occur in this plot).

the $a[110]$ moves and drags the $a[001]$ behind it. For no range of parameters in our idealized model is it possible to decrease $L$.

To illustrate the evolution of the system loop, we consider its motion in the $W$–$L$ plane. A point $\{W, L\}$ in this plane represents a loop with the given shape parameters. From this point, the system will move, via equation (5), towards some neighbouring point. Its velocity vector $\{\dot{W}, \dot{L}\}$ describes the instantaneous direction of the evolution of the system. Because the velocities are functions of the

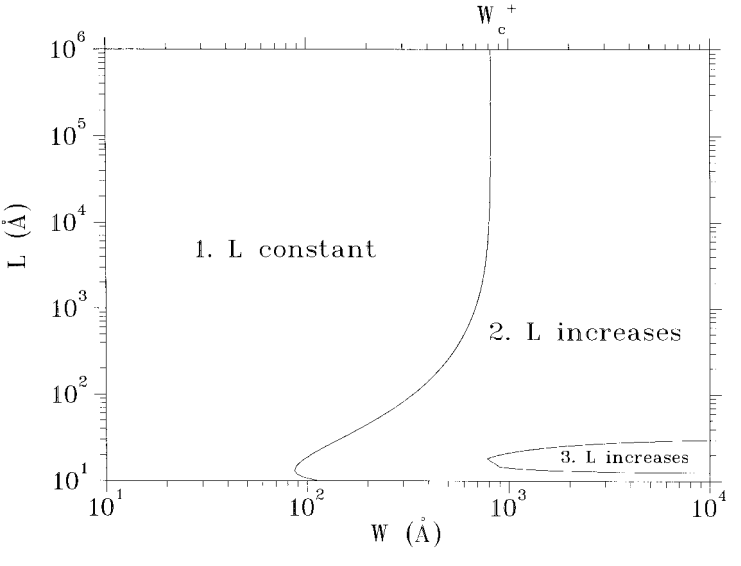


Figure 9. Contours of constant $f_L$, showing different regions of behaviour; region 1, $f_L < -f_P^{a[001]}$, $L$ constant; region 2, $-f_P^{a[001]} < f_L < +f_P^{a[001]}$, $L$ grows; region 3, $f_L > +f_P^{a[001]}$, $L$ increases rapidly.

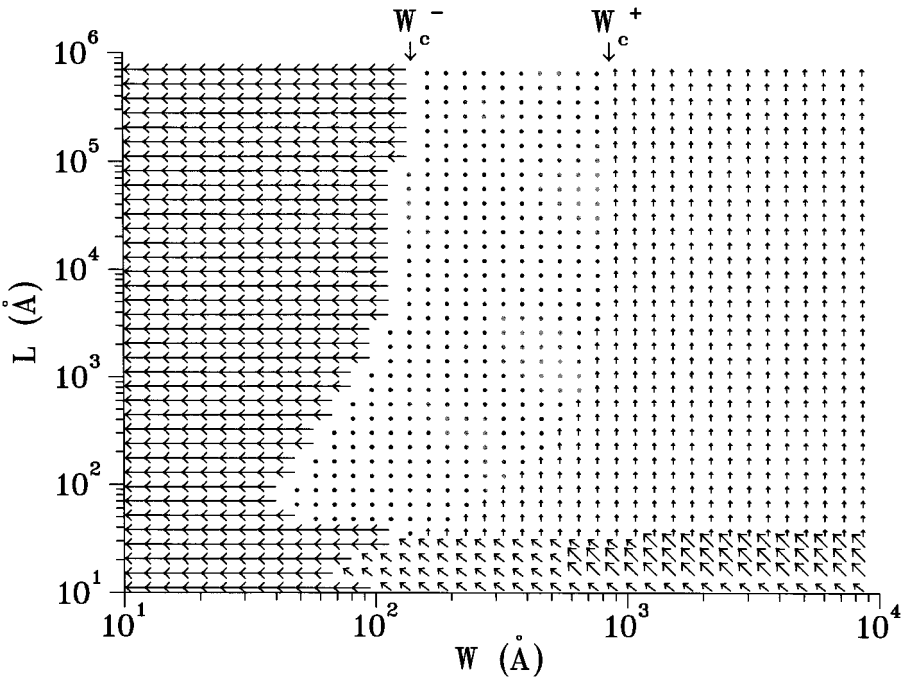


Figure 10. Velocity vectors $\{\dot{W}, \dot{L}\}$ in the $W$–$L$ plane which describe the evolution of any configuration of the type shown in figure 7. At any point in the plane, the vector shows the direction in which the system will evolve.

instantaneous position, each point in the $\{W, L\}$ plane has a determined direction for evolution. Figure 10 illustrates the resulting velocity vectors in the $W$–$L$ plane. The velocity vectors represent tangents to trajectories in the $W$–$L$ plane.

If we consider that an incipient loop starts with small $L$, then relevant trajectories will begin near the $W$ axis in the $W$–$L$ plane, as in figure 11. For small initial values of $W$ (less than about 100 Å), as in trajectory 1, the loop collapses. For moderate initial values of $W$ (100–1000 Å), as in trajectory 2, the system may end up in a static configuration, with $W \approx 300$ Å and $L \approx 100$ Å. For larger initial values of $W$ (greater than 1000 Å), as in trajectory 3, the reaction is downhill, and $L$ freely increases until the $a[110]$ dislocations have swept out of the material, leaving extended $a[001]$ dipoles. In this final state, the dipoles are attractive, but the separation is sufficient that the attraction cannot overcome the frictional stress.

These results are consistent with TEM observations of microstructures following deformation near the knee temperature. Just below the knee, many instances of initial decomposition have been observed where the geometry resembles our idealized geometry (see figure 5 of Srinivasan *et al.* (2000)). These decompositions 'caught in the act' may well correspond to structures near the 'doldrums', where little change in structure is expected (trajectory 2). Just above the knee, many of the observed $a\langle 001\rangle$ dislocations are arranged in dipoles (as shown in figure 7 of Srinivasan *et al.* (2000)). $a\langle 110\rangle$ segments are also seen along with the complete absence of $a\langle 111\rangle$ dislocations, consistent with structures where $L$ extends freely (trajectory 3).

As can be seen in figure 10, $a\langle 001\rangle$ dipoles can form with a distribution of widths depending on the initial value of $W$. The dipoles seen in the experiments are found to

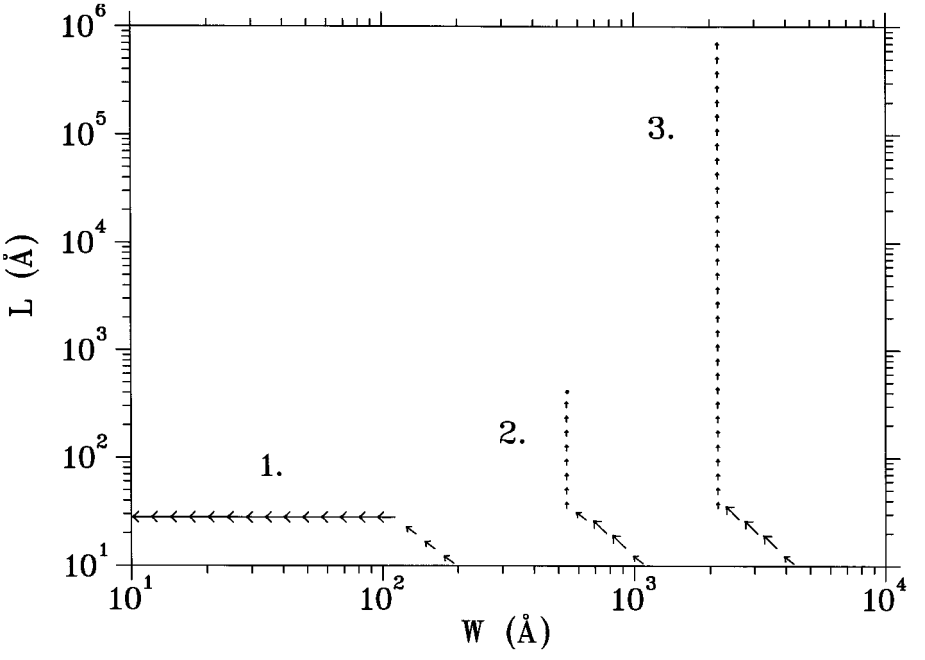


Figure 11. Three sample trajectories based on the equations of motion, equations (5). The three trajectories start with small $L$ and $W = 200$ Å (arrows 1), 1000 Å, (arrows 2) and 4000 Å (arrows 3).

have a distribution of widths as well, the mean size being of the order of 0.06 μm (Srinivasan *et al.* 2000), which is the lower limit for complete decomposition of $a\langle 111\rangle$ dislocations (the formation of extended dipoles) as determined by the present calculations.

As an added consideration, we have investigated the dependence of the 'doldrums' in figure 10, that is the region where the loop would appear not to change shape. The boundaries of this region are defined by the contours in figures 8 and 9. For large $L$, the lower and upper edges of this region are denoted $W_c^-$ and $W_c^+$ in the figure. The equations for $W_c$ are transcendental, but it can be demonstrated analytically that to a very good approximation we have $W_c^+/W_c^- \approx 6$, independent of the elastic constants and frictional stress (but dependent on the Burgers vectors of the products). Thus, while the scale of figure 10 may change somewhat depending on our guesses for the frictional stress, for example, the qualitative aspects of the figure are unchanged, and our general conclusions remain.

## §4. Discussion

The main objective of the preceding sections is to suggest a reason why decomposition of the $a\langle 111\rangle\{110\}$ dislocations does not occur spontaneously at low temperatures, in spite of the fact that decomposition is energetically favoured. This decomposition can be stalled by the formation of a metastable state involving a short-range climb decomposition which places the products into a 'piggyback' configuration. This 'piggyback' structure is indeed lower in energy than the perfect dislocation; but it is metastable with respect to complete decomposition. We find also a natural mechanism by which decomposition is nucleated and proceeds to the formation of unusual deformation microstructure: partially formed decomposition

loops, and long parallel $a\langle 001\rangle$ dislocation dipoles. A simple elasticity analysis explains quite naturally how the loops end up in those structures.

However, having answered those questions, we are still left with at least three serious questions.

(1) The theory and observations seem to show that total and complete decomposition does not occur, in the sense that we see evidence here for a decomposition which involves only a small portion (about 1000–10 000 Å) of the $a\langle 111\rangle$ line at one time. Is it possible to obtain total decomposition? This seems especially relevant in that, for experiments above the knee temperature, *no* $a\langle 111\rangle$ dislocations are present.

Note that, after the formation of the decomposition node as described above, it is the hard-oriented stress (along the [010] direction, for the analysis described in this paper) that imposes a glide force on the $a[110]$ that is possibly responsible, in part, for the complete decomposition of the $a[111]$ dislocation (Srinivasan *et al.* 2000). Also, note that, in the hard orientation, there is no glide or climb force on the $a[001]$ decomposition product.

One possibility here is that the nucleation of decomposition loops may be increasing rapidly at the knee temperature. If this is true, neighbouring decomposition loops can link up; in fact, the energetics would favour such a coalescence. In this way, perhaps much more of the parent can be decomposed.

(2) There is in fact a saddle-point configuration between the metastable state and the decomposed structure. It is tempting to attribute the saddle-point energy to an activation energy for a thermal excitation process. In that case, does the activation energy correspond quantitatively to the knee temperature?

It apparently does not, for two reasons. First, the saddle-point energy appears to be too high. Even given that our simple idealized geometry and use of isotropic theory causes our estimate of the energetics to be systematically too high, the saddle-point energy is still too high to correlate with the observed knee temperature. Second, the controlling factor appears to be the mobility of the $a\langle 110\rangle$ dislocations. This is borne out by pre-straining experiments (see figure 8 of Srinivasan *et al.* (2000)), which indicate that the nucleation of the decomposition is not the rate-controlling factor. Instead, it seems that the ability of the $a\langle 110\rangle$ to pull away from the $a\langle 001\rangle$ is critical to the progression of the decomposition. This suggests that the mobility of $a\langle 110\rangle$ dislocations is strongly temperature dependent, and that it is this temperature dependence which sets the knee temperature, and not the nucleation of the decomposition loop.

(3) What is the role of stoichiometry? Apparently, changes in stoichiometry have significant effect both on the temperature of the transition and on the microstructure observed near the transition. One possibility is that the mechanism by which the piggyback structure is formed involves local climb, and that may have some bearing. In addition, the prevalence of $a\langle 110\rangle$ dislocations is strongly dependent upon stoichiometry. Thus, by the arguments presented above, one would expect stoichiometric deviations to increase the temperature at which the $a\langle 110\rangle$ mobility is sufficiently large to accommodate $a\langle 111\rangle$ decomposition. This reasoning implies that the critical resolved shear stress for $a\langle 110\rangle$ dislocations is strongly temperature dependent. A model for such a dependence has been proposed recently

(Mills *et al.* 1998), and a more detailed account of $a\langle 110\rangle$ behaviour in Ni–44 at.% Al will be presented elsewhere.

Even though the metastable state does not provide the solution to these three unanswered questions, it is not possible to dispense with it. The resulting peculiar structure predicted from assuming it conforms so well to the observed microstructure that there is little doubt of its existence.

## § 5. Conclusions

We show in this paper that there exists a metastable arrangement of products in the reaction $a\langle 111\rangle \rightarrow a\langle 110\rangle + a\langle 001\rangle$ in NiAl. Atomistic calculations show that the metastable state can be formed spontaneously by a local shuffle or climb decomposition. Once formed, the 'piggyback' configuration can glide as a unit, with a restoring force helping to keep it intact. However, if the product lines become separated locally beyond a critical distance, the result is a decomposition loop. Small dislocation loops (less than 100 Å) collapse, large loops (greater than 3000 Å) evolve into dislocation dipoles, and medium loops can fail to evolve further. These results are consistent with detailed observations of the microstructure.

## Acknowledgements

The Clemson authors acknowledge support from the National Science Foundation, Division of Materials Theory. Support for M.J.M. and R.S. was provided by the US Department of Energy under contract DE-FG02-96ER45550. The authors would also like to thank TRIUMF for providing the graphics software used to make the graphs for this paper.

## References

Field, R. D., Lahrman, D. F., and Darolia, R., 1991, *Acta metall. mater.*, **39**, 2951.

Fu, C. L., and Yoo, M. H., 1992, *Acta metall. mater.*, **40**, 703.

Hirth, J. P., and Lothe, J., 1982, *Theory of Dislocations* (New York: Wiley).

Kim, J. T., 1990, PhD Thesis, University of Michigan, Ann Arbor.

Kim, J. T., and Gibala, R., 1991, *High Temperature Ordered Intermetallic Alloys IV,* Materials Research Society Symposium Proceedings, Vol. 213, edited by L. A. Johnson, D. P. Pope and J. O. Stiegler (Pittsburgh, Pennsylvania: Materials Research Society), p 261.

Ludwig, M., and Gumbsch, P., 1995, *Modelling Simul. Mater. Sci. Engng,* **3**, 533.

Mills, M. J., Srinivasan, R., and Daw, M. S., 1998, *Phil. Mag.* A, **77**, 801.

Rao, S. I., Woodward, C., and Parthasarathy, T. A., 1991, *High Temperature Ordered Intermetallic Alloys IV,* Materials Research Society Symposium Proceedings Vol. 213, edited by L. A. Johnson, D. P. Pope and J. O. Stiegler (Pittsburgh, Pennsylvania: Materials Research Society), p. 125.

Schroll, R., Finnis, M. W., and Gumbsch, P., 1998a, *Acta mater.*, **46**, 919.

Schroll, R., Vitek, V., and Gumbsch, P., 1998b, *Acta mater.*, **46**, 903.

Srinivasan, R., Savage, M. F., Mills, M. J., Daw, M. S., and Noebe, R. D., 1996, *Deformation, Fatigue, and Fracture of Ordered Intermetallic Materials,* edited by W. O. Soboyejo, T. S. Srivatsan and H. L. Fraser (Warrendale, Pennsylvania: Metallurgical Society of AIME), p. 325.

Srinivasan, R., Savage, M. F., Daw, M. S., Noebe, R. D., and Mills, M. J., 1998, *Scripta mater.*, **39**, 457.

Srinivasan, R., Brown, J., Daw, M. S., Noebe, R. D., and Mills, M. J., 2000, *Phil. Mag.* A, **80**, 2841.

Yoo, M. H., Takasugi, T., Hanada, S., and Izumi, O., 1990, *Mater. Trans. Japan Inst. Metals,* **31**, 435.